Proceedings of ASME Turbo Expo 2011
GT2011
June 6-10, 2011, Vancouver, British Columbia, Canada

GT2011-45082

ON REMAINING LIFE ANALYSIS OF TURBINE DISKS SUBJECTED TO HIGH THERMAL STRESSES

Vishwas Iyengar, Ph.D.
Southwest Research Institute®
Mechanical Engineering Division
6220 Culebra Road
San Antonio, TX 78238
vishwas.iyengar@swri.org

Stephen James
Southwest Research Institute®
Mechanical Engineering Division
6220 Culebra Road
San Antonio, TX 78238
stephen.james@swri.org

Harold Simmons, P.E.
Southwest Research Institute®
Mechanical Engineering Division
6220 Culebra Road
San Antonio, TX 78238
harold.simmons@swri.org

ABSTRACT

Disk failures can be caused by a number of mechanisms under the turbine operating conditions of high rotational speed at elevated temperatures. It is not uncommon for highly stressed turbine blades and disks to operate at temperatures in excess of 1,000°F, where increased exposure can affect their life. In the past, it has been adequate to analyze the life of these high temperature components using methods which calculate creep life and low cycle fatigue life independently in predicting service hours. More often than not, the parameters included in the creep life model are based on empirical data. Here, a practical methodology is presented to predict the remaining life of a turbine disk that utilizes a combination of Computational Fluid Dynamics (CFD), Finite Element Analysis (FEA) and a creep model. A full three-dimensional CFD analysis is performed on the turbine disks at design and off-design conditions, in order to accurately capture the thermal loads. A detailed FEA is performed on the turbine disk. The stress inputs for the creep life model are based on the stresses obtained from the FEA. A case study is presented that utilizes the proposed methodology. It is found that the methodology is beneficial for the remaining life analysis on highly loaded turbine disks. The accuracy of the methodology is somewhat dictated by the amount of historical operating data that is available.

INTRODUCTION

A turbine disk can fail by a number of mechanisms under the turbine operating conditions, especially during high temperatures and high rotational speed. Numerous references exist for disk failure investigations and the methods used to arrive at varying conclusive results. Some have listed methods that have been developed to predict the life of turbine blades that are subject to high rotational speeds and elevated temperatures. Walls et al. [1] put forward an approach to assess damage tolerance by predicting crack propagation in blades that undergo high cycle fatigue (HCF). Their life prediction system used a boundary integral element (BIE) derived hybrid stress intensity solution. This accounted for transition from a surface crack to corner crack to edge crack. Greitzer [2] developed a turbine blade durability model based on variability in design and operating parameters. The durability life was modeled as limited by thermo-mechanical low cycle fatigue and creep. The study showed that variation in cooling air bulk temperature was most important in setting the variation in blade durability life. Hou et al. [3] used a non-linear finite element method (FEM) to determine the steady-state and dynamic stresses in a turbine, and thereby determine the cause for blade separation at the top fir-tree. The finite element (FE) model incorporated cyclic symmetry, surface-to-surface contact, centrifugal forces from rotation velocity, and a non-uniform temperature distribution. The likely cause of failure was considered to be a mixture of low cycle fatigue (LCF) and HCF.

Other factors - main gas bulk temperature and heat transfer coefficient also affected disk life, but to a lesser extent. FEM models were also used by Witek [4] to evaluate failure of a turbine disk, this time for an aero engine. Here, a non-linear finite element method was utilized to determine the stress state of the disc/ blade segment under operating conditions. High stress zones were found at the region of the lower fir-tree slot, where the failure occurred. Attention of this study was devoted to the mechanisms of damage of the turbine disk. Zhang et al. [5] also performed a similar disk failure investigation for another aero engine failure. Their analysis results show that the accident was caused by lamellar defects in the steel. A comprehensive evaluation of a gas turbine disk is given by Davidson [6].

Most of the use of CFD for multidisciplinary life prediction has been performed on the blades, some are discussed here. CFD methods were employed by Moussavi Torshizi et al. [7] to study fluid flow, stresses, and vibration that lead to fracture in cooling fan blades. In this study, metallurgical and structural analyses on the failed blades did not show any microstructure degradation. The CFD analysis aimed to achieve air velocity distribution around blades, study airflow lines in order to observe probable vortex formation and related problems, and determine pressure-related force over blades. With CFD and FEM results not being conclusive, the probable reason for failure was attributed to the way blades had been fastened. Filsinger et al. [8] calculated dynamic loading of turbine blades using a coupled CFD-FEM analysis. The unsteady pressure imposed on the airfoil contour leads to circumferentially non-uniform and pulsating excitation forces acting on the rotating bladed disk. Results from the analysis were used to investigate vibration behavior in turbocharger turbine, and therefore avoid blade failure.

A plethora of previous multidisciplinary work has been directed toward turbine blades in terms of predicting their life. Some previous work has been done to predict the life of turbine disks, although not all the work is multidisciplinary and comprehensive. There is still a need to obtain accurate thermal loads from flow analysis, which can be used to predict thermal stresses. Those thermal stresses can then be used to predict the remaining life of the disk. Here, a practical methodology is presented to predict the remaining life of a turbine disk that utilizes a combination of CFD, FEA, and a creep type model. The motivation to develop this methodology came from an analysis that was performed to investigate the failure of the first stage disk of a power turbine (PT) in service. Hence, the methodology is presented in form of a case study, where an active turbine disk is reported.

The turbines used for the case study are part of a two-turbine set (Unit I and Unit II). In 2008, Unit I failed with a liberated disk fragment and exhibited multiple cracks in propagation after only ½ of the expected life was expended with less than 500 starts. Unit II disk was inspected in 2009 and found with one crack in propagation, but had not liberated any fragments.

This study aims to address the following specific issues:

- Develop flow/ thermal model for blade root temperature from measurable temperatures and other factors.
- Develop a turbine disk model to predict stresses from rotational speed and temperature gradients.
- Assess the turbine operating condition on failure.

First, in order to obtain boundary conditions for CFD analysis, all the data from the turbine operation is thoroughly analyzed. This forms a good base to simulate the turbine disk operation as accurately as possible. The predicted loads from the CFD analysis are then used to predict the stresses in the FEA. Finally, a life remaining analysis is performed by using the predictions and empirical relations obtained from the CFD and FE analyses.

ASSESSMENT OF TURBINE OPERATING CONDITION

Operating data for the power turbines were transcribed to spreadsheet format for the dates for the two turbines. The following data was evaluated:

- N1: Gas Generator (GG) Speed, RPM
- N2: Power Turbine (PT) Speed, RPM
- T0: Ambient Temp, F
- BCT: Bearing Cool Air, F
- GG-EGT: GG Exhaust Gas Temperature Average, F (T4)
- PT-EGT: PT Exhaust Gas Temperature Average, F
- RCT: Rim Cooling Temperature, F

CFD, based on heat transfer from surrounding environment, is used to numerically solve for disk and blade temperature profile. Thus, boundary conditions from the surrounding environment must be quantified from recorded operating data and thermodynamic calculations for the gas generator and power turbine. In this sub-task, empirical relationships are developed from the data recorded over the period just before Unit I failed. Maximum and average values for recorded data significant to this analysis are presented in Table 1. This data is necessary to clearly define the boundary conditions for the fluid/ thermal model. The entire set of data also contains critical information on component temperatures, vibration, flow, speed, load, and pressure, which are helpful in diagnosing operating problems with all components on the trains. Ambient daily temperature max to min variations for the location are typically less than 20°F and yearly max to min differences are less than about 10°F. Thus, the variations in GG EGT are more related to compression demand rather than ambient conditions.

TABLE 1. SUMMARY OF MAXIMUM AND AVERAGE TEMPERATURES

Unit 1	GG. EGT Ave	PT. Rim Cooling Air	PT. Exhaust Temp	GG Exhaust Pressure (Psi)
Max	1,073 F	957-946	828 F	15.5
Average	1,013 F	955-933	701 F	13.86
Unit 2	**GG. EGT Avg**	**PT. Rim Cooling Air**	**PT. Exhaust Temp**	**GG Exhaust Pressure (Psi)**
Max	1,065 F	~	927 F	15.85
Average	1,009 F	~	799 F	13.78

Projecting trends based on the relations established by the CFD model in Fig. 1, show disk temperature varies between about 975 and 1,015°F for the period tested. The upper value is important in the calculation of disk life, if the unit operates at this condition for a significant portion of its life. Figure 2 shows the trend of disk temperature and stress during the recorded period.

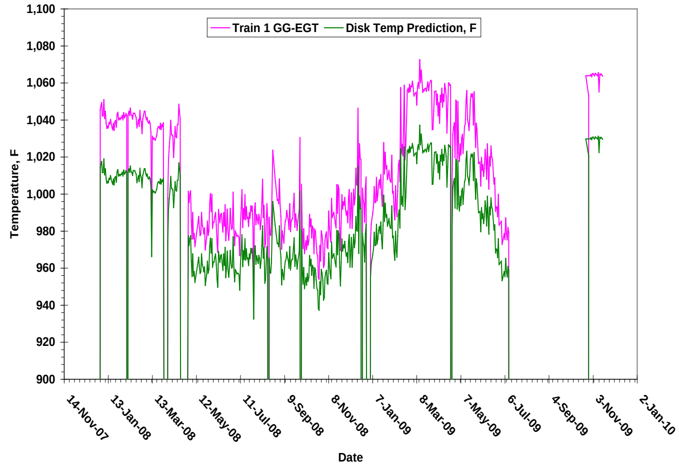

FIGURE 1. PROJECTED TRENDS OF DISK TEMPERATURE BASED ON GG-EGT

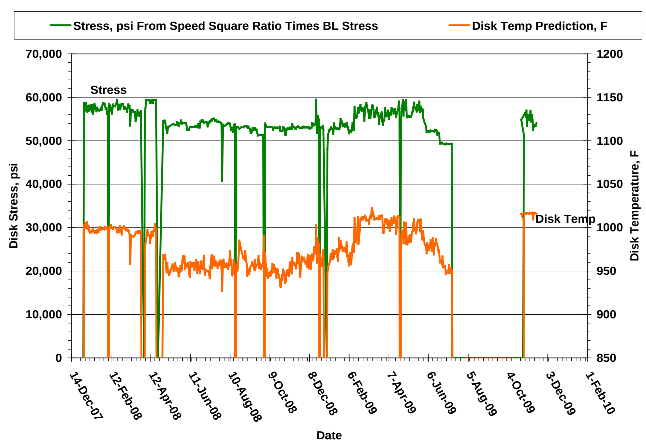

FIGURE 2. TRENDS OF DISK TEMPERATURE AND STRESS DURING THE RECORDED PERIOD

FLOW/ THERMAL MODEL FOR DISK SLOT TEMPERATURE

A full three-dimensional conjugate heat transfer analysis (CHTA) of the turbine-blade configuration is developed in this part of the study. CFD, a branch of fluid mechanics that uses numerical methods and algorithms to solve and analyze problems that involve fluid flows, is used to perform the heat transfer analysis. The CFD analysis is facilitated by ANSYS® CFX™, a commercially available CFD code. CFX meshing tool is used to generate the computational mesh for all cases.

The main objective of this thermal analysis is to determine temperature profiles and regions of high thermal stresses, near the first stage disk. Blade loading due to centrifugal loads, pressure, and temperature loads is of interest. The thermal loading may be determined by solving for the flow properties.

The main gas-flow path through the turbine blade is modeled along with the secondary flow paths near the disk blade attachments. A multi domain approach is used, the main flow path around the rotor blade along with the solid hub, solid rotor blade are modeled. An extensive series of steady state conditions will be evaluated over the range of operation to determine the regions of high thermal stresses, especially near the blade slot failure location in the disk. The result of this study is to establish a set of equations that can be used to predict disk slot temperature relative to exhaust gas temperature (EGT) and rim cooling temperature (RCT).

Figure 3 shows the overall domain used for this analysis. The turbine has 51 number of rotor blades. However, the domain presented here represents 1/51st of the overall turbine section. Rotational periodicity is assumed with the other sections. The computational domain has five different regions- (1) Main flowstream (fluid domain), (2) Upstream cavity (fluid domain), (3) Downstream cavity (fluid domain), (4) Blade (solid domain), and (5) Blade root (solid domain). The computational mesh for each domain is generated independently. When performing a heat transfer problem, the near wall mesh becomes important, as it is responsible for heat transfer. Hence, very fine inflation layers are utilized for the computational mesh near walls that are subject to transfer of thermal properties. Figure 4 shows a close-up of the mesh near the fluid-solid domain interface wall, the inflation layers are visible. The number of elements in the overall computational mesh is approximately 258,000.

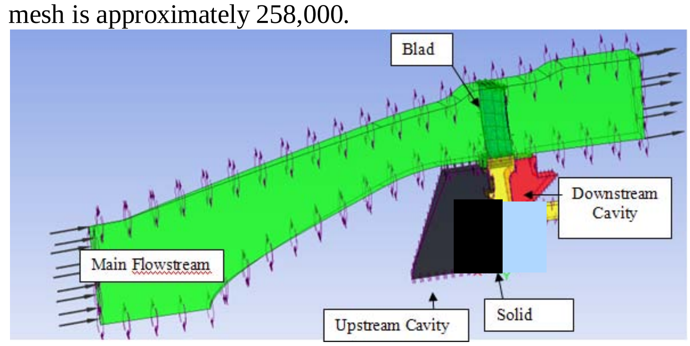

FIGURE 3. OVERALL COMPUTATIONAL DOMAIN USED FOR THE THERMAL ANALYSIS

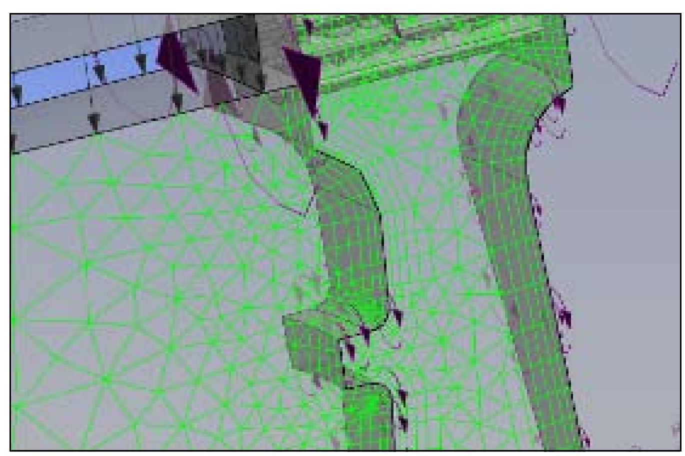

FIGURE 4. CLOSE-UP OF NEAR WALL COMPUTATIONAL MESH SHOWING THE INFLATION LAYERS

At the inlet, the total pressure and temperature conditions are prescribed, and at the outlet, a mass flow rate condition is prescribed. These conditions are obtained from the turbine operating conditions analysis discussed earlier. As per simulation requirements, an initial temperature is necessary for the solid domains. The exhaust gas temperature is given as one of the boundary conditions at the inlet of the computational domain. In the upstream cavity, a stream of cooling air is injected from the previous stage. This rim cooling is supposed to provide cooling air to the hot turbine blade. The gas exhaust temperature is varied along with turbine rotational speed and mass flow rate. The rim cooling temperature is also varied along with the initial condition prescribed in the downstream cavity. Table 2 shows the five cases that were analyzed.

TABLE 2. OPERATING CONDITIONS USED FOR CFD ANALYSIS

CASE	GG EGT (F)	GG Speed (% Design)	PT Speed (% Design)	Mass Flow (%Design)	GG Exhaust Pressure (psi)	PT Exhaust Temp (F)
I	965	98	97	97	12.6	788
II	990	99	99	98	13.2	788
III	1015	100	100	100	13.9	788
IV	1040	101	101	102	14.6	788
V	1065	102	103	103	15.3	788

Figure 5 shows the streamlines originating from the inlet boundary when the EGT is 965°F (Case I). Velocity vectors at a mid-section plane are shown in Fig. 6.

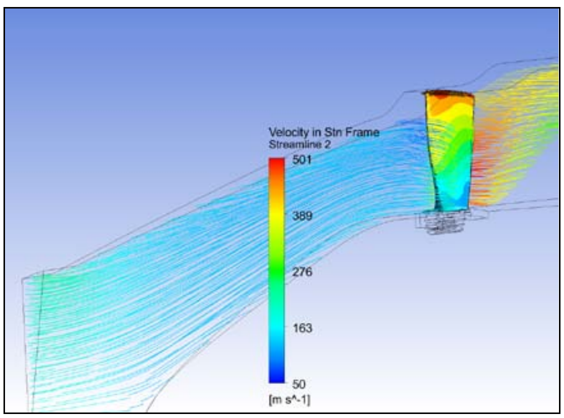

FIGURE 5. STREAMLINES THROUGH THE MAIN FLOWSTREAM DOMAIN FOR 965°F EGT (CASE I)

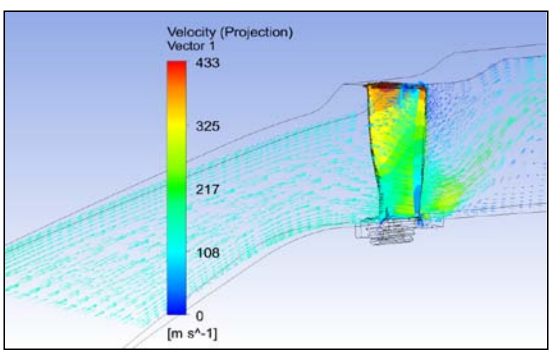

FIGURE 6: VELOCITY VECTORS ON A MID-SECTION PLANE FOR 965^{o}F EGT (CASE I)

The streamlines and velocity vectors provide a means of confirming the magnitude and direction of flow. As expected, the mainline flow turns with the camber on the rotor blade and exits through the outlet boundary. The inlet flow from the upstream cavity enters the main flow stream from the blade disk and then progresses to the outlet boundary. From the velocity vectors it is noticed that the maximum velocity occurs downstream of the blade as the flow tries to turn with the blade.

Figure 7 shows the temperature contours on the blade surface and blade disk surfaces for Case I. The temperature contours on the upstream and downstream cavity periodic surfaces are also shown. For this case, a fairly uniform temperature profile is noticed for the rotor blade. A close-up of temperature distribution near the blade disk is shown in Fig. 8. According to Fig. 8, the temperature near the blade disk is around 947°F when the EGT is 965°F. Table 3 shows the blade disk temperature for all the cases analyzed. These points are plotted in Fig. 9, from which the following empirical relationship for disk rim temperature is deduced as a function of EGT:

$$\text{Disk Rim Temp } (^{o}\text{F}),\ t = 0.841\ \text{EGT} + 135 \qquad (1)$$

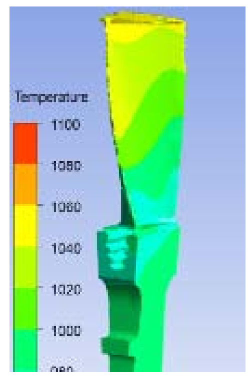

FIGURE 7. TEMPERATURE CONTOURS ON THE BLADE SURFACE AND DISK FOR 965°F EGT (CASE I)

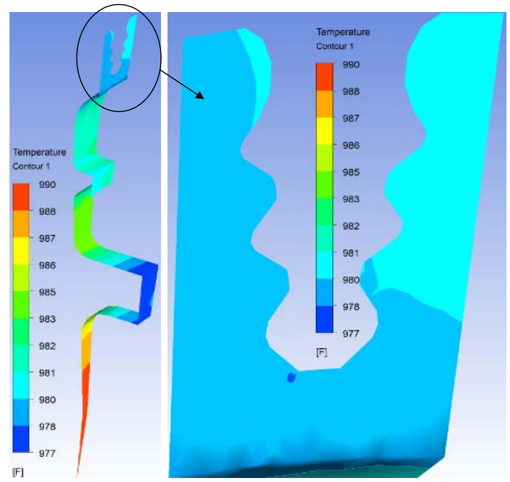

FIGURE 8. TEMPERATURE CONTOURS AT THE BLADE DISK NEAR THE LOCATION OF FAILURE FOR 1,280°F EGT (CASE I)

TABLE 3. SUMMARY OF DISK TEMPERATURE FOR THE VARIOUS OPERATING CONDITIONS

CASE	GG EGT (oF)	GG Exhaust Gas Pressure (psi)	PT Exhaust Temp (F)	Disk Temp (F)
CASE I	965	12.6	788	947
CASE II	990	13.2	788	968
CASE III	1015	13.9	788	989
CASE IV	1040	14.6	788	1010
CASE V	1065	15.3	788	1031

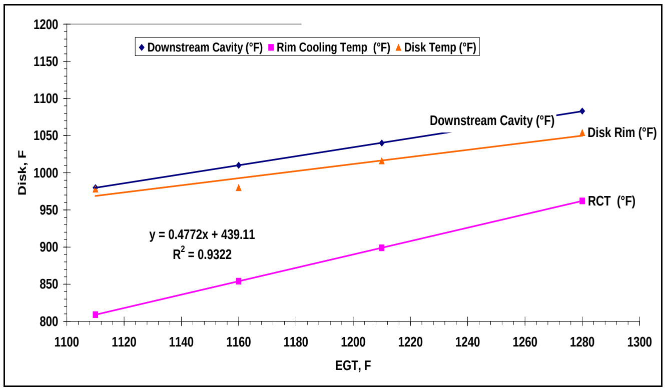

FIGURE 9. PREDICTED DISK RIM TEMPERATURE COMPARED TO SURROUNDING GAS TEMPERATURES

TURBINE DISK MODEL OF STRESS FROM CENTRIFUGAL LOADING

The geometry of the turbine disk is developed with measurements taken from solid parts. The blades were weighed and detailed geometry developed, using white-light scanning technology (Fig. 10). A stress analysis was performed using the commercially available ANSYS® FEA code.

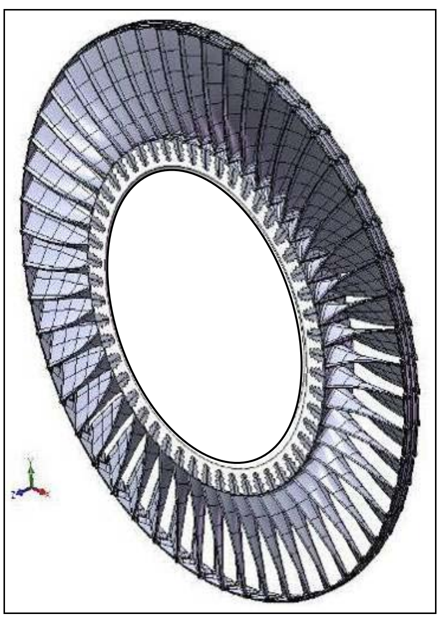

FIGURE 10. MODEL OF DISK AND BLADES

In order to reduce the calculation load, a pie section of the full-scale solid model was generated, as seen in Fig. 11. The pie-section corresponds to a cyclic section of the entire model and comprises of a section of the turbine hub and one blade.

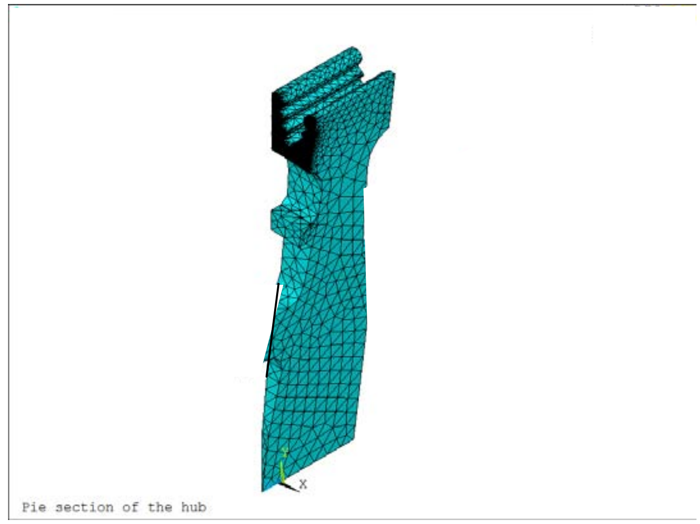

FIGURE 11. DETAIL OF PIE SECTOR MODEL OF BLADE ROOT ATTACHMENT

A cyclic symmetry analysis was employed. A component or assembly is cyclically symmetric, if it has repetitive patterns that are centered about an axis. This analysis conserves time and CPU resources by solving the behavior of a single symmetric sector. Using the single-sector solution, the response behavior of the full circular component can be constructed. ANSYS® Mechanical™ was used to perform the cyclic symmetry analysis. To have an accurate representation of the stresses at the fir-tree root attachment section, these faces were refined with a high density mesh as seen in Fig. 12. The other sections of the model used a coarse mesh.

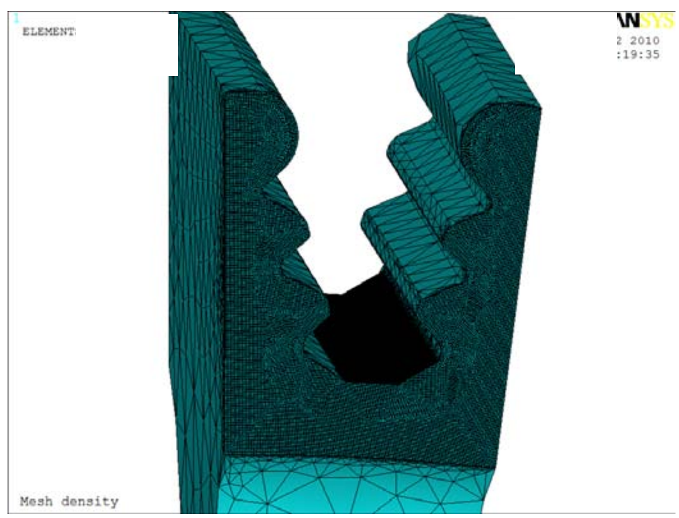

FIGURE 12. MESH REFINEMENT AT THE ROOT OF THE BLADE-HUB INTERFACE

Metallurgical studies show that the failure likely initiated in the hub. The purpose of the finite element analysis is to determine the stress developed in the fir tree of the hub. When the disk assembly rotates, the blades generate centrifugal force. To avoid intense calculation, the three-dimensional blade model is simplified and approximated as a lumped point mass. The point mass was concentrated at the center of gravity location of the blade and represents the actual mass and inertia of the blade. Variation in stress was observed along the axial direction and although it may not be fully representative of a three-dimensional blade, this approximation was assumed sufficient for this analysis. Future analyses may need to include a full three-dimensional blade model for more blade representative stress results.

As the turbine disc rotates, only some of the faces at the fir-tree section experience centrifugal loading. These faces are connected to the point mass using rigid mass less links. Figure 13 illustrates this arrangement.

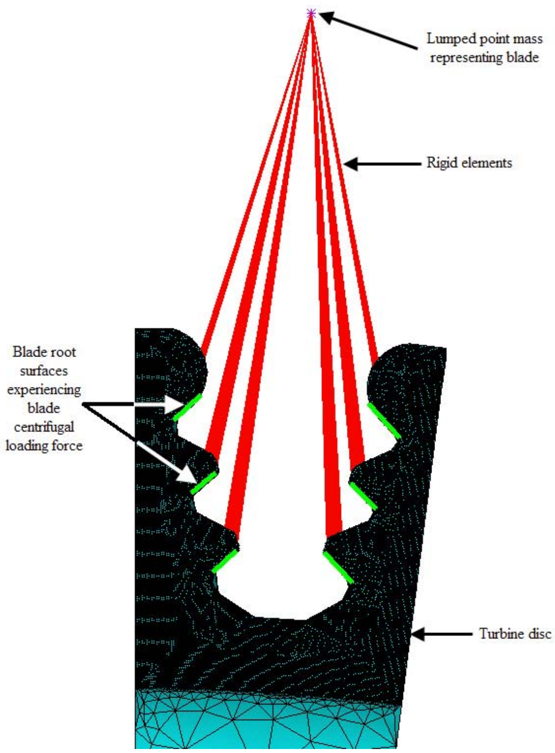

FIGURE 13. FIR-TREE SECTION OF THE TURBINE DISC SHOWING POINT MASS AND RIGID LINKS

The design rotational velocity was applied. The disk was modeled using the mechanical properties of A- 286 material, as shown in Table 4. The rigid links were assigned a very low density (~ $1x10^{-10}$ lb/in^3) so that they do contribute to the overall mass of the model.

TABLE 4. MECHANICAL PROPERTIES FOR A-286 USED IN THE MODEL

A286 Mechanical Properties	
ρ, lb/in3	0.283
E, psi	29x106
Poisson’s Ratio	0.29

There are several scenarios to evaluate in assessing the life time effects of stresses acting on the first stage disk. The first scenario to consider is the prospect for failure by creep. Loads from two different sources are considered; one is the external load due to rotational centrifugal forces (CF), the other load source is due to the internal strains that result from thermal gradients. In a creep situation, the internal strains tend to relax, so that long-term creep damage will only result from externally applied loads. The cyclic effects of both types of load need to be considered in any fatigue related life analysis.

Figure 14 shows a close up of the tangential (hoop) stresses developed in the fir-tree section of the turbine hub. A peak stress of about 50 ksi is observed at about 0.5 inches inside of the outer edge of the disc. It should be further noted that the maximum stress locations are consistent with the failure locations. This implies that the loading effects are accounted for correctly.

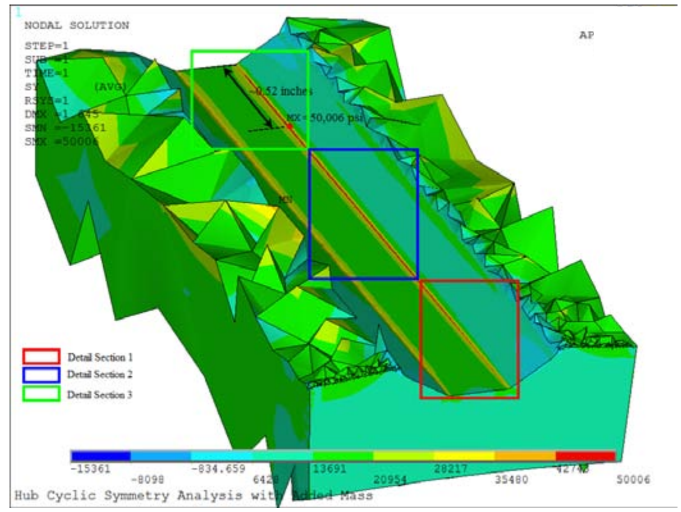

FIGURE 14. PREDICTED STRESSES FOR COMBINED BLADE AND DISK MODEL UNDER CF LOAD ALONE

Based on experience, the disk rim below the blade slot experiences hoop strain and expands both due to CF and thermal loads while the disk rim and blade root outside the blade slot only expands due to thermal strain. The differences of temperature, coefficient of expansion, and stress between these two regions will cause the effective slot width to expand and contract as different transient conditions are experienced. The blade roots simply slip outward as the slots expand owing to the angle of the root contact surfaces; the effect of this slippage will have minimal effect on root loading and stress at the failure location. When the slots contract, however, the blade root must be pulled back by adverse wedging action that causes friction to amplify both normal and sliding forces. This action has resulted in galling damage in the dovetail attachments of many different engines that further exasperates the adverse loading problem. If galling is found in bearing surfaces, it may result in higher stresses than predicted by a conventional bladed disk model. A separate paper by the same authors on the effects of non-uniform blade root friction and sticking on disk stresses can be found in reference [9].

FAILURE MODE ANALYSIS

The time to predict creep-rupture failure (TR) of A-286, for the disk stress and temperature predictions at each daily recorded point during the test period, was evaluated with creep material failure data from Radhakrishnan [10]. Figure 15 shows Radhakrishnan’s rupture life data trends from A-286 test data over a wide range of temperatures and stresses

A creep damage fraction was calculated by dividing each sample period (24 hours) by TR; a very small fraction resulted for each point. These were summed and inverse taken to predict total life after adjustment for the recorded period; a creep life of 3.4 million hours is predicted by this classical method, or approximately 55 times the life experienced.

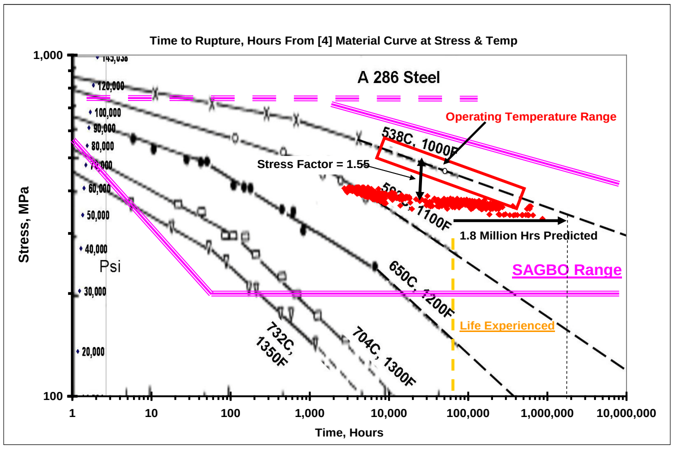

FIGURE 15. CREEP DATA ON A-286 FROM V. M. RADHAKRISHNAN [10]. SUPERIMPOSED ARE PREDICTED STRESS LEVELS FOR THE RECORDED PERIOD

Superimposed on the creep data in Fig. 15 are calculated disk stresses (red points) as a function of predicted life; these have been adjusted so that the sum of cumulative damage results in failure in the experienced 7.6 years of operation. To accomplish this foreshortened life, a factor of 1.55 was applied to calculation of stress; this is equivalent to reducing strength by a factor of 1.55 due to the effects of Stress Assisted Grain Boundary Oxidation (SAGBO) and/or Type II Hot Corrosion. It would not be unusual for a manufacturer to apply a factor of 10 on life or a factor of 1.25 on stress to compensate for any ignorance in creep properties or the operating service that might be imposed on the turbine resulting in a quoted life in the order of 300,000 hours for normal service.

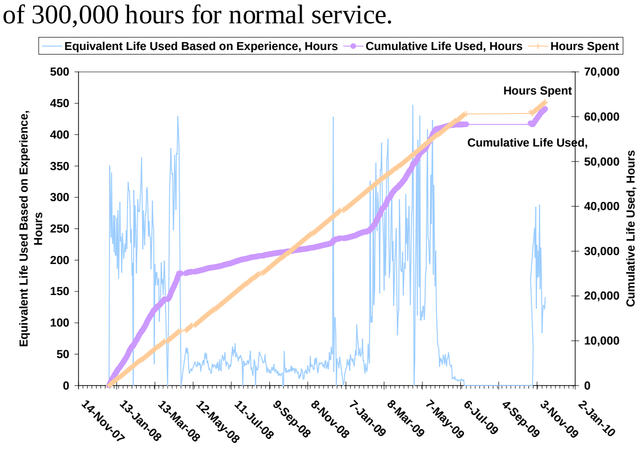

FIGURE 16. TREND OF CREEP LIFE EXPENDED BASED ON THE RECORDED PERIOD

Further life reduction by additional life factor of 2 or material properties reduction by 1.24 is not justifiable without further assessment of other causes. Thus, it can be concluded that the observed failure is not likely caused by creep rupture alone.

An illustration of the creep failure algorithm for each sample period is shown in Fig. 16. In this figure, the creep damage factor (Sample Period/TR) is adjusted by the ratio of life experienced (7.6 years) divided by the recorded period (1.53 years) and plotted as equivalent hours expended on the left axis. The summation of life expended and life spent is shown on the right axis; these values converge at the failure.

The potential for cyclic stress causing fatigue damage is evaluated by plotting predicted stress range vs. experienced start cycles on the fatigue data from MIL Handbook [11]. Trains 1 and 2 each experienced 324 and 436 starts or attempted starts respectively over their lifetimes. The stress range experience during a typical stop/startup cycle should be between about 50,000 psi and 70,000 psi, if the unit is shut down in a controlled way; emergency shutdowns may result in significantly greater stress ranges. Superimposing this stress range in orange at 1,000 cycles (lowest available) in Fig. 17, shows that the experienced cyclic stress levels and number of cycles are well below an extrapolated line for the appropriate R= 0 (min/max) stress ratio curve for shutdown events. Thus, it can be concluded that the observed failure is not caused by conventional low cycle fatigue (LCF) alone.

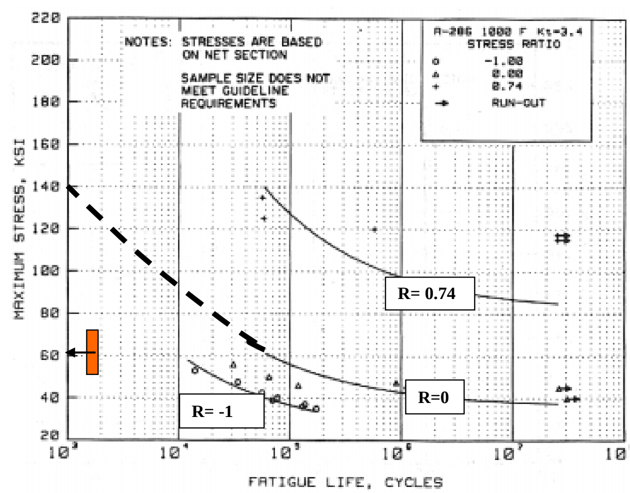

FIGURE 17. SN DIAGRAM FOR A-286 AT 1,000 F WITH KT FACTOR = 3.4 (STRESS CONCENTRATION FACTOR) [11]

The usual approach for estimating the combined creep and fatigue is to add the life consumed by both mechanisms. Clearly, the sum of creep rupture life consumed plus fatigue life consumed is still a very small number. A more rheological simulation of creep-fatigue (“Hold Time Fatigue”) based on strain range testing of A286 at 593°C (1,100°F) in air is presented in Fig. 18. It is worth noting that A-286 can have a ‘notch-ductility trough’ at around 1,000°F (severity depends on heat treat and alloy content). This data compares gas phase embrittlement (GPE), resulting from intergranular oxygen penetration with tests done in vacuum. It is clear, that the cyclic disk stress effects occur in air at elevated temperature. Crack initiation and propagation was intergranular. The frequencies tested in Fig. 18 are two orders of magnitude greater than the frequency of shutdown events (324 cycles/66700 hours/60 = 0.00009 cpm) which lends uncertainty on how well this data applies (see dashed line), but it would seem reasonable that the disks are exposed to oxygen and this mode of failure is likely.

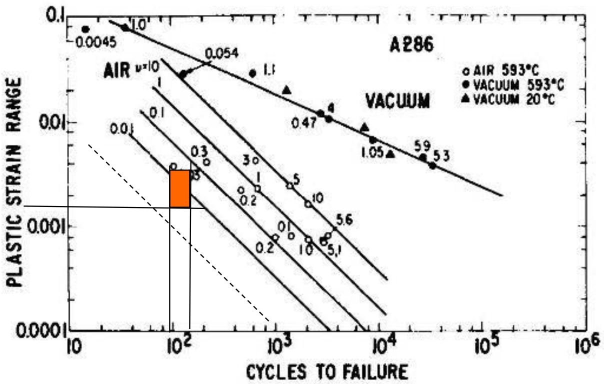

FIGURE 18. PLASTIC STRAIN RANGE VS. FATIGUE LIFE FOR A286 IN AIR AND VACUUM AT 593°C (1,100°F) [12]; NUMBERS ADJACENT TO TEST POINTS INDICATE FREQUENCY, CPM; THE DASHED LINE REPRESENTS INCREASING CYCLIC PERIOD TOWARD THAT EXPERIENCED IN THE UNIT

Stress Assisted Grain Boundary Oxidation (SAGBO) involves the embrittlement along the grain boundaries due to oxygen diffusion which causes cracking. It has been reported that SAGBO is responsible for much of the intergranular cracking that has occurred in INCONEL alloys 718 and 706 at elevated temperatures; these are iron based alloys similar to A 286 with high nickel content. SAGBO occurs in INCO 908 when Tensile stress >200 Mpa (29,000 psi), temperature between 450 – 850°C (840- 1,500°F), and >0.1 ppm O2 conditions that are met, as outlined by the pink boundaries in Fig. 15.

CONCLUDING DISCUSSION

Herein, a comprehensive thermal and mechanical analysis is conducted to predict the remaining life of a turbine disk and also to provide an insight into the root cause of it failure. A multidisciplinary approach was proposed and a real-life case study was used as a test case. The investigation conducted can be divided into the review of the disk operation data, structural and thermal simulations and various failure modes. The following concluding remarks can be made:

- The evidence and data explored herein clearly indicate that neither creep-rupture nor fatigue acting alone or combined in a normal way are responsible for the turbine disk failures experienced.
- The projected strain range experienced during stop/ startup cycles and reported number of cycles is consistent with the Hold-Time Fatigue mechanism when exposed to air.
- It can be said that disk operates in the range of conditions consistent with SAGBO damage, which is consistent with contributing to the Hold-Time Fatigue mechanism.
- Thermal simulations show the disk temperature is not expected to exceed 1,020°F, well below the type II range for nickel-based alloys.
- All failure mechanisms explored are sensitive to temperature, with damage rates generally increasing temperature. The converse of this is that decreasing temperature will generally increase life, although there are some exceptions. Almost all materials show relatively constant strength properties with increasing temperatures up to some point, and then substantial decline in properties at higher temperature. For A 286, this limit is about 1,000°F for yield strength, creep, and fatigue.
- Data is not available to quantify increased life with reduced temperature for SAGBO or for Hot Corrosion in iron-based alloys. Experience with other alloys has shown that significant improvement in life should be expected if operating temperature can be limited to below a specific threshold.
- Although some under prediction is observed with the presented methodology, the disk life prediction method provided herein as an operating guide to minimize excessive life consumption due to creep-related mechanisms. The accuracy of the methodology is somewhat dictated by the amount of historical operating data that is made available.

ACKNOWLEDGEMENTS

The authors would like to acknowledge the contributions of Dr N. Sastry Cheruvu, Southwest Research Institute for his valuable insight into this topic.

REFERENCES

[1] Walls, D. P., deLaneuville, R. E., and Cunningham, S. E., 1997, "Damage Tolerance Based Life Prediction in Gas Turbine Engine Blades Under Vibratory High Cycle Fatigue," Journal of Engineering for Gas Turbines and Power, Volume 119, Issue 1, pp. 143-146.

[2] Greitzer, E. M., 2004, "Probabilistic Analysis of Turbine Blade Durability," Massachusetts Institute of Technology, Department of Aeronautics and Astronautics, Massachusetts Institute of Technology.

[3] Hou, J., Wicks, B. J., and Antoniou, R. A., 2002, "An Investigation of Fatigue Failures of Turbine Blades in a Gas Turbine Engine by Mechanical Analysis," Engineering Failure Analysis, Vol 9 (2), p.201-211.

[4] Witek, L., 2006, "Failure Analysis of Turbine Disk of an Aero Engine," Journal of Engineering Failure Analysis, Vol 13, Issue 1, p.9-17.

[5] Zhang, D., and Tao, C. H., 1998, "Investigation of a Turbine Disk Failure," Journal of Engineering Failure Analysis, Volume 5, Number 3, pp. 229-234.

[6] Davidson, D. L., "Gas Turbine Disk-blade Attachment Crack," Journal of Failure Analysis and Prevention Volume 5, Number 1, 55-71.

[7] Moussavi Torshizi, S. E., Yadavar Nikravesh, S. M., Jahangiri, A., 2009, "Failure Analysis of Gas Turbine Generator Cooling Fan Blades," Engineering Failure Analysis, 16 (5), p.1686-1695.

[8] Filsinger, D., Szwedowicz, J., and Schäfer, O., 2002, "Approach to Unidirectional Coupled CFD–FEM Analysis of Axial Turbocharger Turbine Blades," Journal of Turbomachinery, Volume 124, Issue 1, pp. 125-131.

[9] Simmons, H. R., and Iyengar, V., 2011, "Effect of Non-Uniform Blade Root Friction and Sticking on Disk Stresses," Proceedings of the ASME Turbo Expo 2011, Vancouver, Canada.

[10] Radhakrishnan, V. M., 1986, "Rupture Life of Materials Obeying Exponential and Power Law Creep," Transactions ISIJ, Vol. 26.

[11] MIL-HDBK-5H, 1 December 1998, Page 6-13.

[12] Woodford, David A., 2005, "Gas Phase Embrittlement and Time Dependent Cracking of Nickel Based Superalloys," NACE International, Paper No. 05418.